

SUBJECT: Addition of "Mascons" in BCMTAP and
a Preliminary Analysis of their
Effects on Orbit Determination
Case 310

DATE: July 31, 1969

FROM: J. T. Findlay

ABSTRACT

Lunar mass concentrations ("mascons") have been implemented in the Tracking Analysis Program (BCMTAP) as mass points. Modifications to both the equations of motion and the variational equations have been completed.

A limited orbit determination analysis was conducted to show the effects of "mascons" as modeling errors. Pseudo Doppler data were generated using a spherical Moon model in addition to the "mascons". These data were then processed with only the spherical Moon modeled. Thus the state vector offsets and corresponding residual patterns obtained are directly attributable to the unmodeled "mascons".

First, the effects of five highly probable mass concentrations on a low orbit LO III type trajectory were investigated. For the particular orbit the "mascons" located at Nectaris and Humorum are dominant. One and two orbit solutions were obtained. The two rev fit resulted in a much larger position offset which was almost entirely out-of-plane. Trajectory solutions are presented in Table III and residual plots are presented in Figures 1-3.

Secondly, the effects of a single "mascon" were evaluated to provide a set of residuals for further analysis which will attempt to reconstruct the magnitude and location of the unmodeled "mascon". A sequence of five polar orbits were used, the ground tracks of which were essentially evenly spaced to encompass a $\pm 10^\circ$ band of longitude to either side of the "mascon". State vector offsets and residual signatures obtained are presented herein.

An attempt was made to evaluate the effects of different tracking geometry for one of the polar orbits. The residual pattern was essentially unchanged even though a different O.D. solution resulted. For the polar orbit study larger state offsets occurred for those spacecraft orbits which were nearer the "mascon" as expected. However, the false large plane change that occurred when the spacecraft flew

(NASA-CR-112621) ADDITION OF MASCONS IN
BCMTAP AND A PRELIMINARY ANALYSIS OF THEIR
EFFECTS ON ORBIT DETERMINATION (Bellcomm,
Inc.) 30 p

N79-71645

Unclass

11760

00/12

directly over the "mascon" was unexpected. It was shown that this resulted because the polar orbit was being viewed edge-on and the observable (Doppler range difference data) is somewhat insensitive to small plane changes. In fact, a simulated plane-in-the-sky orbit (normal to the Earth-Moon line) which flew directly over a "mascon" resulted in an almost totally in-plane correction as it should have.

Earth-Moon geometry for the particular epoch selected gives rise to the apparent unequal effects of the "mascon" on trajectories which pass essentially equidistant from the imbedded mass-point. More of the acceleration due to the "mascon" is reflected in the Doppler observable for those trajectories which pass to the west of the "mascon" since the selenographic longitude of the Earth is approximately 6.5° West. This biases the orbit determination results.

BELLCOMM, INC.

955 L'ENFANT PLAZA NORTH, S.W.

WASHINGTON, D. C. 20024

SUBJECT: Addition of "Mascons" in BCMTAP
and a Preliminary Analysis of
their Effects on Orbit Determination - Case 310

DATE: July 31, 1969

FROM: J. T. Findlay

MEMORANDUM FOR FILEIntroduction

Studies conducted by Mueller and Sjogren at JPL have shown some rather convincing evidence that there are areas of large mass concentration located beneath the Moon's surface. High degree and order spherical harmonic gravity potential models, particularly an 11th order field derived by LRC, yield elevation contours which are also indications of "mascons". The actual number, shape, size and location of these "mascons" will not be known for some time. Additionally, an analysis such as conducted by JPL gives no information as to the existence of lunar far side "mascons".

As a first approximation it was decided to simulate the dynamical effects of these mass concentrations in BCMTAP using a mass point formulation. The capability to solve for the location and magnitude of these mass points was not considered. Together with the spherical harmonic potential model already available in BCMTAP, the addition of the mass points constitutes a hybrid lunar potential model.

Formulation of Mass Point Equations

The equations of motion in subroutine ACCEL have been modified to include the accelerations exerted on the spacecraft by the mass points as follows:

$$\ddot{X} = \sum_{i=1}^N -\mu_i \frac{(X - X_i)}{\Delta^3}$$

$$\ddot{Y} = \sum_{i=1}^N -\mu_i \frac{(Y - Y_i)}{\Delta^3}$$

$$\ddot{Z} = \sum_{i=1}^N -\mu_i \frac{(Z - Z_i)}{\Delta^3}$$

$$\text{where } \Delta = \left((X - X_1)^2 + (Y - Y_1)^2 + (Z - Z_1)^2 \right)^{1/2},$$

X, Y, Z are the inertial coordinates of the spacecraft in Selenocentric Mean of 1950 coordinates,

X_1, Y_1, Z_1 are the inertial coordinates of the i^{th} mass point,

and μ_1 is the mass of the i^{th} mass point.

The μ_1 are input in parts per million of the total mass of the moon. The inertial coordinates for the i^{th} mass point are obtained by rotating the Selenographic coordinates into Selenocentric Mean of 1950. The Selenographic location is determined as follows.

$$X_s = R_1 \cos \phi \cos \lambda$$

$$Y_s = R_1 \cos \phi \sin \lambda$$

$$Z_s = R_1 \sin \phi$$

where R_1 is the radial distance to the mass point measured from the Moon's center

and ϕ, λ are latitude and longitude of the mass point respectively.

When mass points are included the mass used in the central body term for the Moon is reduced automatically by an amount equal to the sum of the added "mascons".

When integrating the equations of motion in BCMTAP a trajectory tape is written for use in interpolation of the state vector of the spacecraft, e.g., when integrating the variational equations or processing tracking data. Given a function and its first and second derivatives at two points, the interpolation routine evaluates the function at intermediate points. For interpolation on position, no additional modifications are necessary since the accelerations must

necessarily be modified to include the effects of the "mascons". However, to provide for adequate velocity interpolation the mass point "jerk" contributions must be included. The additions are as follows:

$$\ddot{\dot{X}} = \sum_{i=1}^N -\mu_i \frac{(\dot{X} - \dot{X}_i)}{\Delta^3} + 3\mu_i \frac{(X - X_i)}{\Delta^5} r$$

$$\ddot{\dot{Y}} = \sum_{i=1}^N -\mu_i \frac{(\dot{Y} - \dot{Y}_i)}{\Delta^3} + 3\mu_i \frac{(Y - Y_i)}{\Delta^5} r$$

$$\ddot{\dot{Z}} = \sum_{i=1}^N -\mu_i \frac{(\dot{Z} - \dot{Z}_i)}{\Delta^3} + 3\mu_i \frac{(Z - Z_i)}{\Delta^5} r$$

where

$$r = (X - X_i)(\dot{X} - \dot{X}_i) + (Y - Y_i)(\dot{Y} - \dot{Y}_i) + (Z - Z_i)(\dot{Z} - \dot{Z}_i)$$

The selenocentric mass point velocities are obtained by rotating the selenographic velocities into the inertial frame. The selenographic velocities are given by:

$$\dot{X}_i = -Y_i \cdot \Omega_m$$

$$\dot{Y}_i = X_i \cdot \Omega_m$$

$$\dot{Z}_i = 0$$

where $\Omega_m = 2.662 \times 10^{-6}$ rad/sec, rotational rate of the Moon.

In BCMTAP the state transition matrices are obtained by integration of the variational equations. The state transition matrix is used to relate errors in the state vector at some time, t , to state errors at epoch, t_0 . The elements of the matrix are first order partial derivatives, e.g., $\partial x(t)/\partial x(t_0)$. Thus the variational equations were modified to adequately reflect the mass point effects in the state transition matrix. The variational equations are as follows:

$$\ddot{\phi} = \begin{bmatrix} 0 & I \\ G & 0 \end{bmatrix} \phi$$

where Φ is the state transition matrix relating variations in state at time t to errors in state at epoch, t_0 ;

0 is a 3×3 null matrix;

I is a 3×3 identity matrix;

and G is a 3×3 symmetric matrix whose elements are partial derivatives of the spacecraft accelerations with respect to position.

The following quantities were added to the G matrix to represent the effects of the "mascons".

$$\frac{\partial \ddot{X}}{\partial X} = \sum_{i=1}^N \frac{-\mu_i}{\Delta^3} + 3\mu_i \frac{(X - X_i)^2}{\Delta^5}$$

$$\frac{\partial \ddot{X}}{\partial Y} = \frac{\partial \ddot{Y}}{\partial X} = \sum_{i=1}^N 3\mu_i \frac{(X - X_i)(Y - Y_i)}{\Delta^5}$$

$$\frac{\partial \ddot{X}}{\partial Z} = \frac{\partial \ddot{Z}}{\partial X} = \sum_{i=1}^N 3\mu_i \frac{(X - X_i)(Z - Z_i)}{\Delta^5}$$

$$\frac{\partial \ddot{Y}}{\partial Y} = \sum_{i=1}^N \frac{-\mu_i}{\Delta^3} + 3\mu_i \frac{(Y - Y_i)^2}{\Delta^5}$$

$$\frac{\partial \ddot{Y}}{\partial Z} = \frac{\partial \ddot{Z}}{\partial Y} = \sum_{i=1}^N 3\mu_i \frac{(Y - Y_i)(Z - Z_i)}{\Delta^5}$$

$$\text{and } \frac{\partial \ddot{Z}}{\partial Z} = \sum_{i=1}^N \frac{-\mu_i}{\Delta^3} + 3\mu_i \frac{(Z - Z_i)^2}{\Delta^5}$$

Preliminary Orbit Determination Analysis Using "Mascons"

A limited study was conducted to evaluate the effect of mass points as modeling errors on "state only" orbit determination solutions. First the resulting state updates due to five "mascons" for one and two orbit fits were evaluated. Secondly, residuals resulting from a single "mascon" were obtained for use in a forthcoming analysis which will attempt to reconstruct the magnitude and location of the mass-point from the accelerations implied by the time derivative of the fitted Doppler residuals.

Five "Mascon" Study

Pseudo tracking data were generated for two stations assuming a spherical Moon with five "mascons". The "mascons" considered were Mare Imbrium, Mare Serenitatis, Mare Nectaris, Mare Crisium, and Mare Humorum. Preliminary masses and locations were obtained from Dr. P. Gottlieb of JPL and are given in Table II. These "mascons" were numbered among the seven presented by Mueller & Sjogren in their paper in "Science". Only two, Crisium and Nectaris, are located within the band of latitude defined by the ground track of the satellite for this inclination. The ground track for the trajectory used in this study is presented in Figure 4. The state vector used is presented in Table I. Also shown are the corresponding osculating orbital elements. The nominal state vector corresponds to the low orbit LO III trajectory.

Whereas the five "mascons" were simulated it can be seen from Figure 4 that the effects of Nectaris and Humorum are dominant. At closest approach a rough estimate of the accelerations indicates that Nectaris would yield 3.5 times the peak acceleration produced by Humorum. This is approximately the difference seen in the residuals. The other "mascons" produce accelerations at their respective closest approaches which are negligible compared to the Nectaris "mascon".

Tracking data were generated for two orbital passes at a 60 second sample rate with Woomera as the master, or two-way, station and Goldstone in a three-way, or slaved, mode. Doppler range-difference data were used. These data were processed against a spherical Moon model to isolate the effects of the "mascon". Any state vector offset then can be considered as being in error from the actual spacecraft trajectory. For the particular epoch and tracking configuration chosen only the two-way station had visibility during the second pass.

State vector updates for the one and two pass solutions are presented in Table III in inertial coordinates as well as in the local vertical frame. The local vertical frame is defined as u (radial), v (down-range) and w (cross-track). Corresponding orbital element changes are also presented. Again, these updates result primarily from the Nectaris and Humorum "mascons". The two pass fit results in a larger position offset than the one rev solution. This increase is almost entirely out-of-plane and corresponds to the larger change in the ascending node. The two pass solution also results in a larger period, and corresponding semi-major axis, change.

Residual signatures are presented in Figures 1 through 3. Figure 1 shows the direct effect of the "mascons" on the two-way (CC3) and three-way (C3) observables. These residuals result from the first iteration through the data and do not reflect any state update. The points of closest approach to both the Humorum and Nectaris "mascons" are evident from the residual plots. These occur approximately 1500 and 2800 seconds respectively for the first rev. The closest approaches to Humorum and Nectaris are indicated on the residual plots. Final residual plots for the one-pass and two-pass solutions are shown in Figures 2 and 3. For comparison purposes, quantization noise for real data at this sample rate would be approximately 0.0015 fps. Thus, final residuals are well above the noise level for actual MSFN tracking data and "mascons" of this magnitude would show up in the fit residuals. The single "mascon" study discussed in the next section was conducted to determine how well the magnitude and location of such a "mascon" could be reconstructed from the residuals.

Single "Mascon" Study

A more extensive study was conducted using a single "mascon" of 40 ppm located 50 km beneath the surface on the lunar equator at zero longitude. Five non-consecutive polar orbits were used as the reference trajectories. Table IV lists the five nominal states at the processing epochs. These orbits are separated by approximately 5° in descending node covering the region of $\pm 10^\circ$ of longitude.

Pseudo tracking data were generated with a spherical Moon model in addition to the "mascon" to represent the lunar gravity field. For each of these orbits data were generated for one master and one slaved station. These data were then processed against a spherical Moon to obtain the least squares estimate of state. All solutions obtained were for single are processing and should be construed as deviations from the actual spacecraft trajectory produced by the unmodeled "mascon".

Table V shows the state vector updates in inertial and local vertical coordinates as well as corresponding changes to the osculating orbital elements due to the "mascon" as a modeling error. The residuals obtained are presented in Figures 4A-9B. The A figures are the residuals resulting from the "mascon" prior to any state update. The B figures are the final fit residuals. The sixth solution, trajectory 5A, was made to ascertain the effect of different station geometry by re-running the fifth trajectory using Goldstone in lieu of Madrid as the two-way station, keeping Ascension as the three-way. The resulting offsets obtained from the Madrid-Ascension combination were larger than that obtained using Goldstone-Ascension, e.g., a three times larger inclination change. However, the final fit residuals for both 5 and 5A are essentially the same.

From Table V one can see the variation in the offset state and orbital elements as the satellite ground track approaches the zero meridian containing the "mascon". The maximum deviations from trajectory 3 are expected since the satellite is much closer to the imbedded mass point. That this also gives the largest plane change was somewhat unexpected since the orbit passes essentially over the "mascon". Also initially unexpected but apparent from Table V is the lack of symmetry between the OD solutions for any two trajectories which are essentially equidistant from the "mascon", e.g., between trajectories 1 and 5 (5A) which pass approximately 10° East and West of the mass point respectively. This lack of symmetry is particularly apparent when comparing residual plots for the trajectories.

The large plane change for trajectory 3 is due partially to the fact that the spacecraft didn't exactly pass over the "mascon". Whereas an attempt was made to pass directly over the mass-point, the particular reference trajectory used actually passed approximately 0.1° East of the "mascon". This causes an acceleration normal to the orbit, the maximum value of which would be approximately $5 \times 10^{-5} \text{fps}^2$. However the acceleration would tend to increase the inclination and decrease the node which is in the direction of the offset. This of itself would not be enough to effect the large plane change which resulted.

For the most part, the large plane change results from the fact that the orbit is being viewed essentially edge-on and the observable (Doppler shift) is somewhat insensitive to small plane changes. For example, a change in inclination is essentially a rotation about the Earth-Moon line. The zero Doppler shift point is hardly affected and at the limbs,

where essentially the total velocity is being measured, the small differences are essentially masked. Contrast this situation to a plane-in-the-sky type orbit which is essentially normal to the Earth-Moon line. For this situation a small Doppler shift results and any changes in the orbital inclination produce, percentage-wise, a significant change in the Doppler observable. Therefore, the orbit is not free to discard the effects of a modeling error into the out-of-plane direction. In fact, a plane-in-the-sky orbit was simulated. The "mascon" was located at 90° East longitude and the polar orbit flew directly over it. The state update resulting from the modeling error was almost entirely an in-plane correction.

The lack of symmetry in the OD solutions has been ascribed to Earth-Moon geometry. This can best be seen not by looking at the orbit solutions themselves but by comparison of residual plots. The orbit determination program does the best it can in the presence of a modeling error to minimize these residuals. Thus the phenomena which cause the residuals to be so apparently different are also primarily responsible for the different OD solutions. Factors which can introduce differences in the residuals are; (a) non-symmetry in the reference trajectories relative to the "mascon", (b) tracking station geometry and (c) Earth-Moon geometry.

Comparison of the results of trajectories 5 and 5A show that station geometry can have an influence on the resulting orbit but minimal effect on the Doppler residuals. Yet residuals for both 5 and 5A are significantly different than those obtained for trajectory 1. Non-symmetry in the reference trajectories can not produce residual differences of the magnitude observed. Trajectory 5(5A) has a longitude at closest approach of 9.7° West whereas trajectory 1 passes the "mascon" approximately 9.9° East. This accounts for only 3.8 percent of the difference in acceleration due to the "mascon". The residual plots indicate that the effects of the "mascon" on trajectory 5(5A) are approximately 2 times greater than that for trajectory 1.

The apparent differences in the accelerations due to the "mascon" for these trajectories is due to Earth-Moon geometry. For the particular epochs selected the selenographic latitude and longitude of the Earth are both approximately -6.5° . These values correspond to essentially maximum values of lunar libration in latitude and longitude respectively. Considering only the longitudinal libration one can approximate the effects of the "mascon" on the Doppler observable for both trajectories 1 and 5(5A). Since the two reference trajectories are essentially symmetric the maximum acceleration produced

by the "mascon" on both can be considered the same (0.00535 fps^2). However, since the earth is in the western hemisphere at this time the component of this acceleration along the Earth-Moon line is greater for trajectory 5(5A) than for trajectory 1. The angle between the acceleration due to the "mascon" and the Earth-Moon line for trajectory 1 is approximately 74.5° . The corresponding angle for trajectory 5(5A) is 61.5° . This results in a factor of 1.8 times larger acceleration projected along the Earth-Moon line for trajectory 5. The component normal to the Earth-Moon line doesn't contribute to the Range difference observable and is essentially unmeasured.

The fact that the residual plots for trajectories 2 and 4 show essentially the same "mascon" influence is somewhat misleading. Here, the bias produced by the westward orientation of the Earth is offset by the lack of symmetry in the ground track for these two trajectories. Trajectory 2 actually crosses the equator at 4.5° East whereas trajectory 4 has a longitude at closest approach of -5.3° . This difference alone causes a 16.7 percent larger acceleration for trajectory 2. When Earth-Moon geometry is taken into account, trajectory 4 should result in about 18 percent larger acceleration along the Earth-Moon line. This is approximately the difference observed in the residual plots.

Referring again to Table V some explanation is necessary regarding the changes to ω and f for trajectories 2 and 3. For the circular reference orbits used in the study the OD program defines perilune argument as selenographic latitude at epoch and defines true anomaly to be zero. When eccentricity is changed by greater than $1\text{E-}5$ values are computed for both ω and f . Both trajectories 2 and 3 resulted in sufficient change in eccentricity to redefine ω and f .

Conclusions

Lunar mass concentrations have been simulated in BCMTAP as mass points. Both the equations of motion and the variational equations have been modified and the check out completed.

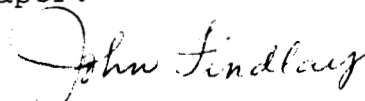
The effect of "mascons" as modeling errors on orbit determination solving for state only has been studied. Residual signatures obtained for the various O.D. solutions are characteristic of a "mascon" modeling error. The residuals from the single "mascon" study will be used to attempt to reconstruct the magnitude and location of the unmodeled "mascon".

The state offsets resulting from the unmodeled "mascon" were found to increase for trajectories in which the spacecraft was closer to the "mascon" as expected. However, the direction of the offsets were not as expected, in particular, the plane change for Run 3 which flew directly over the "mascon". This resulted because the observable was rather insensitive to small plane changes for the edge-on orbits simulated. A simulated plane-in-the-sky orbit resulted in essentially an in-plane solution for an unmodeled "mascon" located directly under the spacecraft's orbit.

Apparent asymmetrical effects of the "mascon", noticeable in the state offsets as well as the residual plots, were attributed to Earth-Moon geometry and were shown to be maximum for the particular epoch selected.

Acknowledgements

The author would like to acknowledge the contribution of Mr. R. D. Weiksner (2014) who encoded the "mascon" logic and generated the data for this paper.


J. T. Findlay

2014-JTF-bsb

Attachments
Tables I-V

TABLE I

Selenocentric Mean of 1950 State Vector

X	=	-6,685,791.1338 ft.
Y	=	753,854.2322 ft.
Z	=	145,070.43963 ft.
\dot{X}	=	-283.7476049 fps
\dot{Y}	=	-3632.2877296 fps
\dot{Z}	=	-3371.7477033 fps
EPOCH	August 30, 1967	
	20 hrs. 54 min. 58.51 sec.	

Selenographic Orbital Elements of Date

Semi-Major Axis, (a)	6,457,408.2 ft.
Eccentricity, (e)	0.04346
Inclination, (i)	20.8969 deg.
Argument of Ascending Node, (Ω)	63.856 deg.
Argument of Perilune, (ω)	354.375 deg.
True Anomaly, (f)	193.425 deg.
Altitude of Perilune, (h_p)	474,345.9 ft.
Altitude of Apolune, (h_a)	1,035,680.6 ft.
Orbital Period, (T_p)	2.1765 hrs.

TABLE II

Summary of "Mascons" Used

	Magnitude (ppm)	Depth Below Lunar Surface (km)	Latitude (deg)	Longitude (deg)
Mare Imbrium	22	100	34	-17
Mare Serenitatis	16	100	25	18
Mare Crisium	12	100	18	57
Mare Nectaris	9	100	-14	33
Mare Humorum	3	50	-22.5	-39

TABLE III

CHANGES IN STATE AND ORBITAL ELEMENTS DUE TO 5 "MASCONS"

Number Orbital Passes	Selenocentric Mean of 1950						Local Vertical Coordinates						Totals	
	ΔX (ft)	ΔY (ft)	ΔZ (ft)	$\dot{\Delta X}$ (fps)	$\dot{\Delta Y}$ (fps)	$\dot{\Delta Z}$ (fps)	Δu (ft)	Δv (ft)	Δw (ft)	$\dot{\Delta u}$ (fps)	$\dot{\Delta v}$ (fps)	$\dot{\Delta w}$ (fps)	Δpos (ft)	Δvel (fps)
1	165.6	121.4	616.8	-0.463	0.229	-0.341	-164.1	-518.5	354.7	0.493	0.096	-0.362	649.3	0.619
2	-391.6	-860.3	1936.2	-0.378	-0.068	0.249	251.6	-660.5	2035.3	0.363	-0.094	0.263	2154.6	0.458

Number Orbital Passes	Δa (ft)	Δe	Δi (deg)	$\Delta \Omega$ (deg)	$\Delta \omega$ (deg)	Δf (deg)	Δh_p (ft)	Δh_a (ft)	ΔT_p (hrs)
1	-85.9	-.166E-4	0.0037	0.0099	0.0099	-0.0237	25.2	-197.0	-0.434E-4
2	228.7	0.806E-5	0.0055	0.0469	-0.0796	0.0302	166.7	290.7	0.116E-3

TABLE IV

REFERENCE TRAJECTORIES FOR SINGLE "MASCON" STUDY

Traj. No.	Epoch	Selenocentric Mean of '50 State						λ^* (deg)
		X (ft)	Y (ft)	Z (ft)	\dot{X} (fps)	\dot{Y} (fps)	\dot{Z} (fps)	
1	31 Aug. 1967, 01:20:00	-1317848.4	343947.08	5912003.4	2039.8264	-4881.7859	738.86456	10
2	31 Aug. 1967, 11:20:00	-617268.16	-1219239.2	5910995.5	2283.0259	-4771.7631	-745.7041	5
3	31 Aug. 1967, 19:00:00	-2329799.5	3176421.9	4613917.9	1139.7774	-4012.3481	3337.9273	0
4	1 Sept. 1967, 05:00:00	-1875180.0	1776656.0	5489399.3	1667.7587	-4634.036	2069.6744	-5
5 (5A)	1 Sept. 1967, 13:00:00	-1401887.8	549225.74	5877057.2	1995.9952	-4867.012	931.10588	-10

 λ^* Approximate longitude of descending node

TABLE V

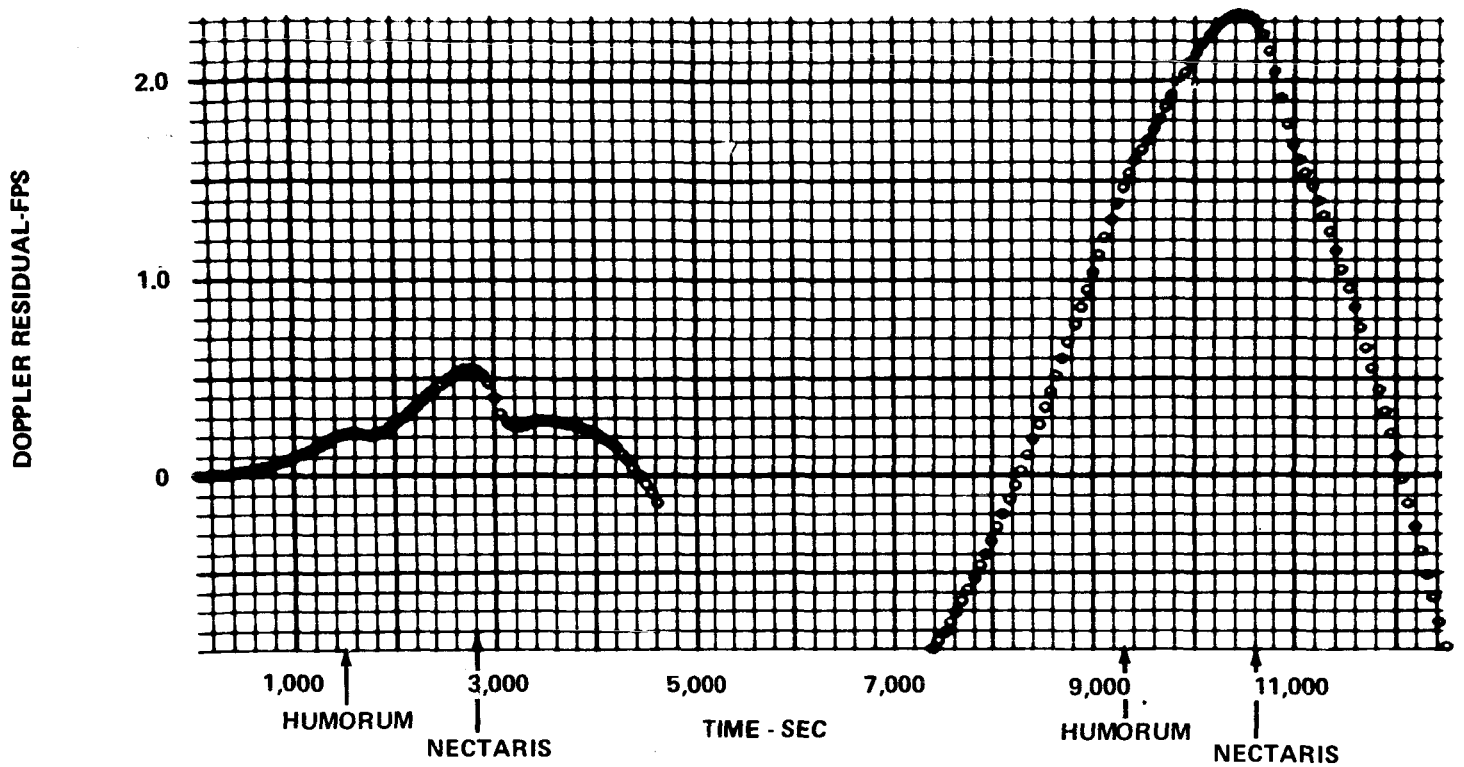
State Vector Updates Resulting From Single "Mascon" As Modeling Error

Traj. No.	Selenocentric Mean of '50 Coordinates						Local Vertical Coordinates					
	ΔX (ft)	ΔY (ft)	ΔZ (ft)	$\dot{\Delta X}$ (fps)	$\dot{\Delta Y}$ (fps)	$\dot{\Delta Z}$ (fps)	Δu (ft)	Δv (ft)	Δw (ft)	$\dot{\Delta u}$ (fps)	$\dot{\Delta v}$ (fps)	$\dot{\Delta w}$ (fps)
1	1032	- 271	1103	0.153	0.346	-1.138	835	795	1013	-1.123	-0.415	0.076
2	2335	- 728	2320	-4.300	0.019	-3.019	2170	1322	2215	-2.510	-1.429	-4.389
3	16423	2220	13370	1.025	-2.411	-9.402	5094	10176	17998	-8.818	-3.829	-1.685
4	7205	3862	1411	-5.383	-1.791	-0.643	192	-563	8274	0.550	-0.370	-5.671
5	- 6837	-4319	450	2.710	1.803	-1.763	1636	1454	-7799	-2.175	-0.936	2.846
5A	- 3072	-2244	899	2.123	1.474	-1.376	1381	1052	-3503	-1.692	-0.788	2.257

Corresponding Changes To Osculating Orbital Elements

Traj. No.	Δa (ft)	Δe	Δi (deg)	$\Delta \Omega$ (deg)	$\Delta \omega$ (deg)	Δf (deg)	ΔT_p (hrs)
1	727	--	0.0088	-0.0037	0.0075	--	0.000356
2	1089	0.000244	0.0110	-0.050	130.34	229.67	0.000534
3	1397	0.000598	0.0716	-0.155	184.56	175.54	0.000684
4	-475	--	0.0158	-0.0978	-0.0053	--	-0.000232
5	1134	--	-0.0486	0.0632	0.0137	--	0.000555
5A	967	--	-0.0166	0.0375	0.0099	--	0.000474

WOM - PSEUDO DATA (CC3)



GDS - PSEUDO DATA (C3)

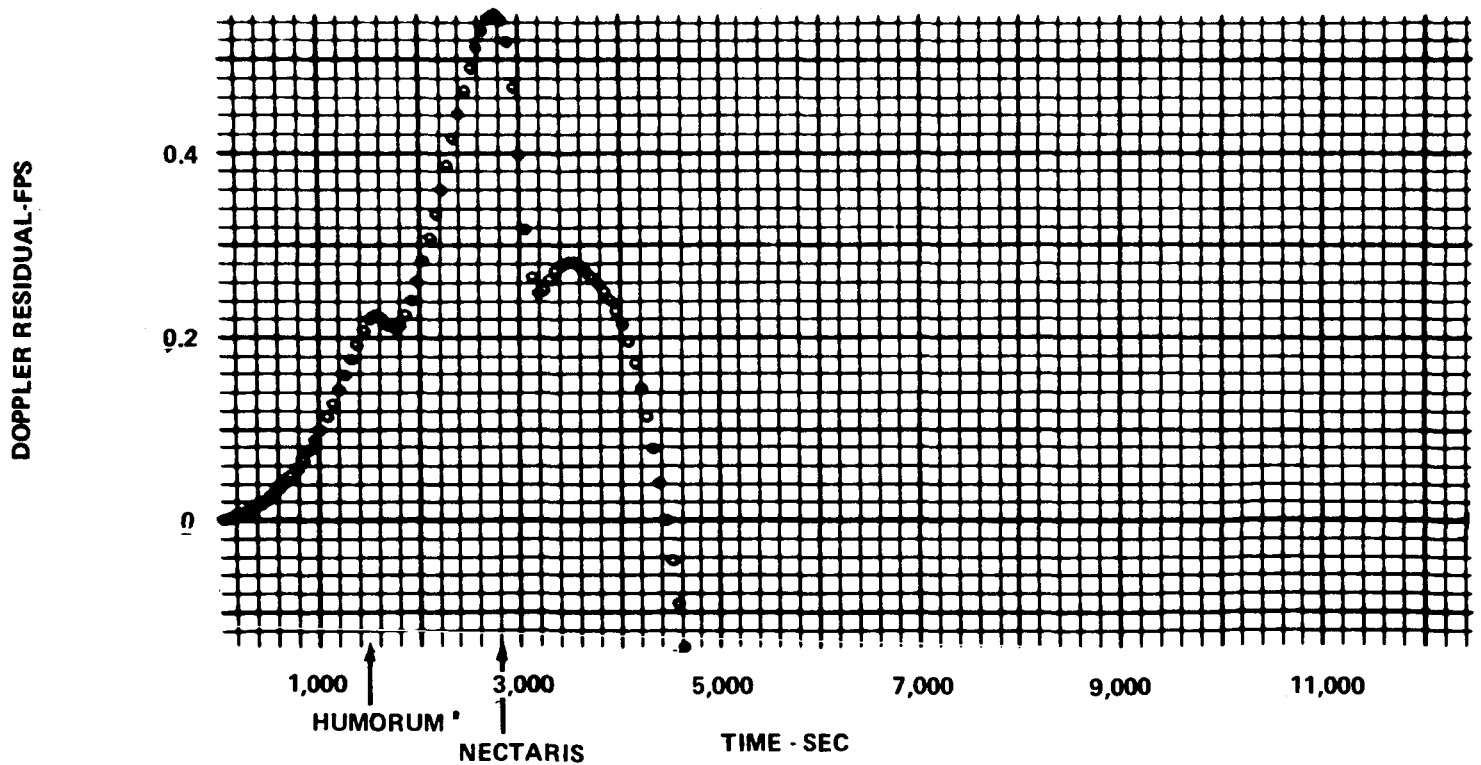
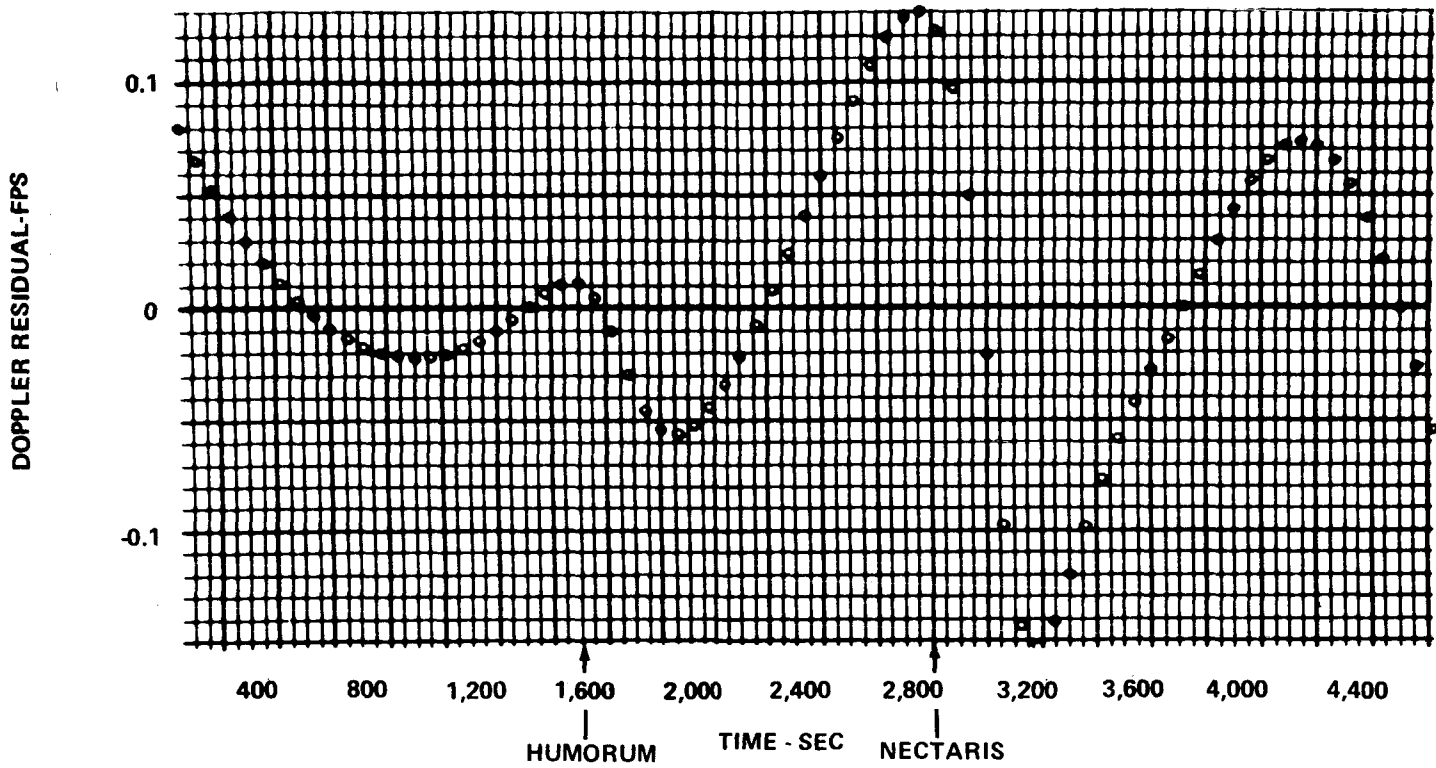


FIGURE 1 - EFFECT OF 5 UNMODELED "MASCONS" ON DOPPLER OBSERVABLE OVER TWO ORBITS

WOM - PSEUDO DATA (CC3)



GDS - PSEUDO DATA (C3)

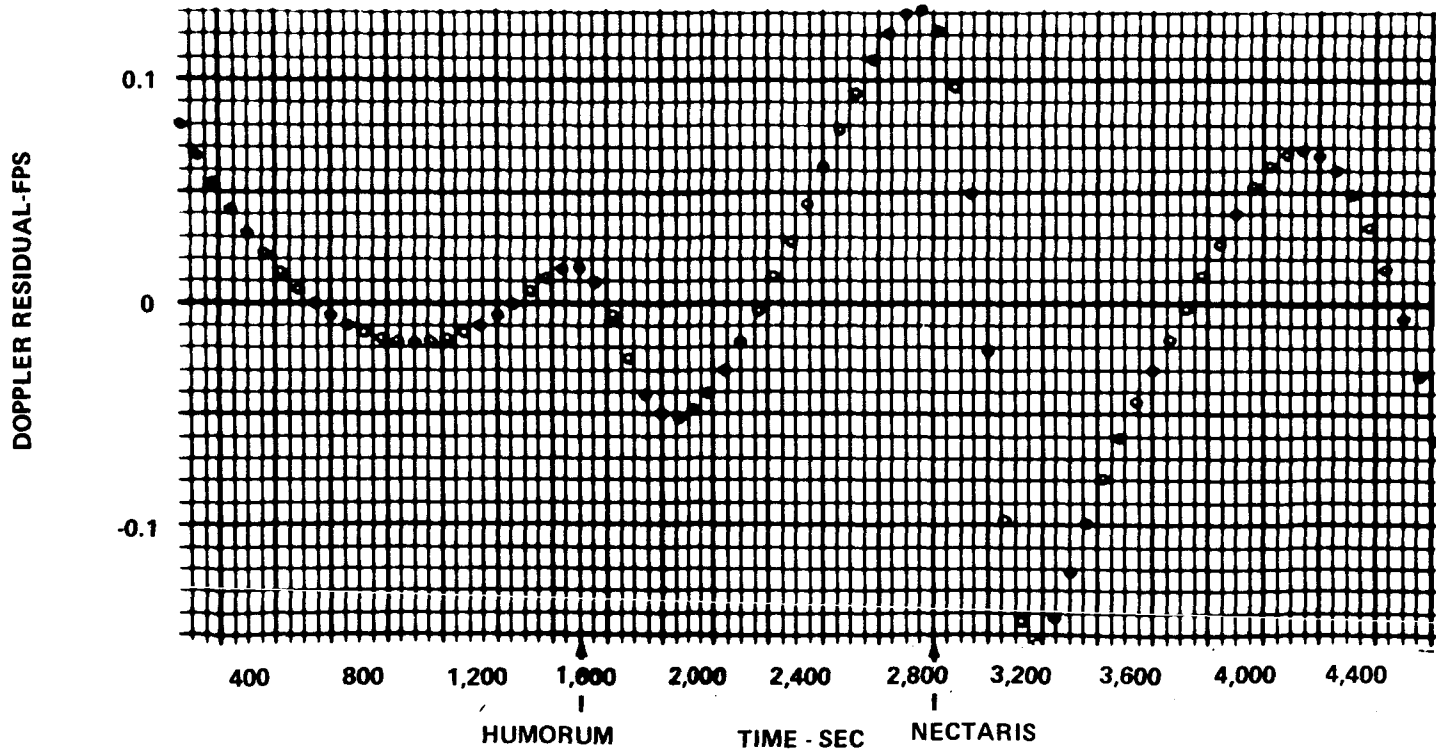
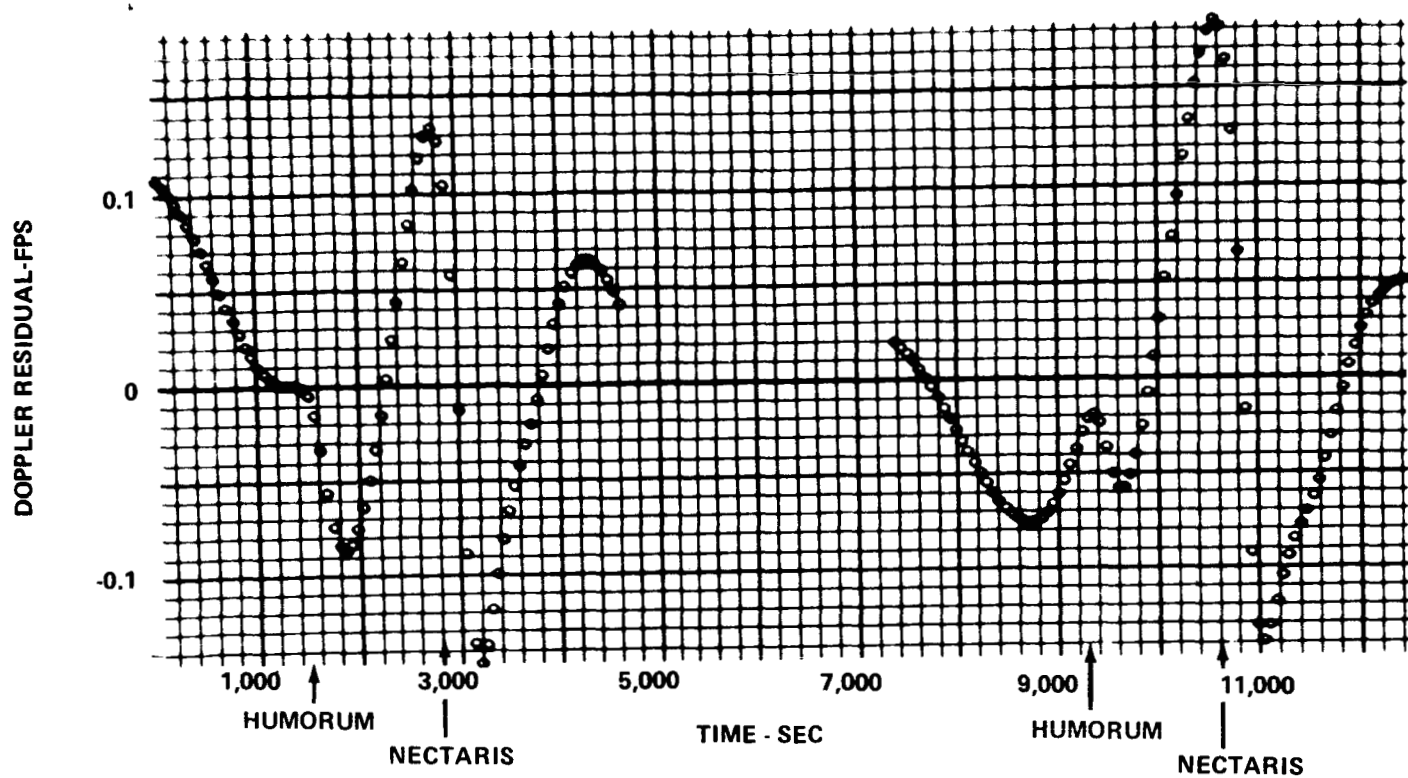


FIGURE 2 - RESIDUAL SIGNATURES DUE TO 5 UNMODELED "MASCONS"
(SINGLE ORBIT FIT)

WOM - PSEUDO DATA (CC3)



GDS - PSEUDO DATA (C3)

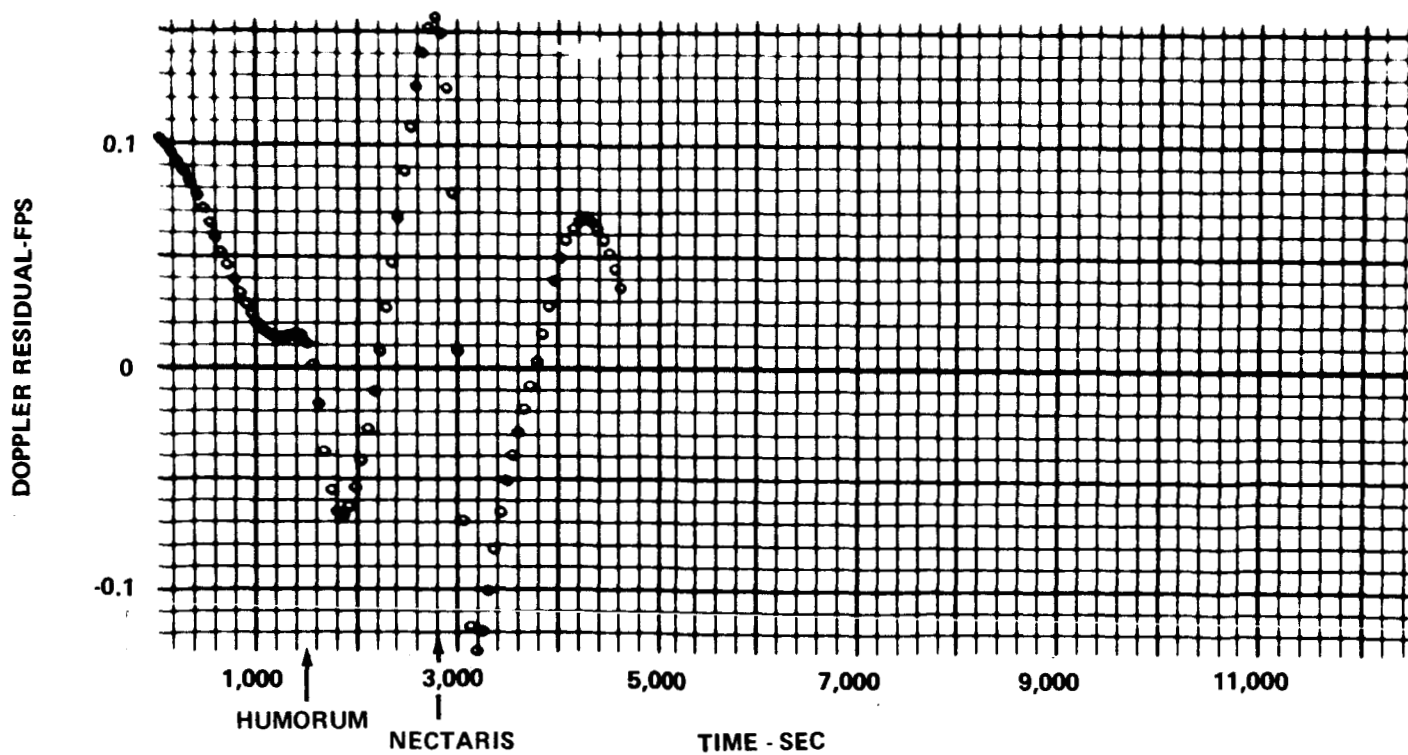


FIGURE 3 - RESIDUAL SIGNATURES DUE TO 5 UNMODELED "MASCONS"
(TWO ORBIT FIT)

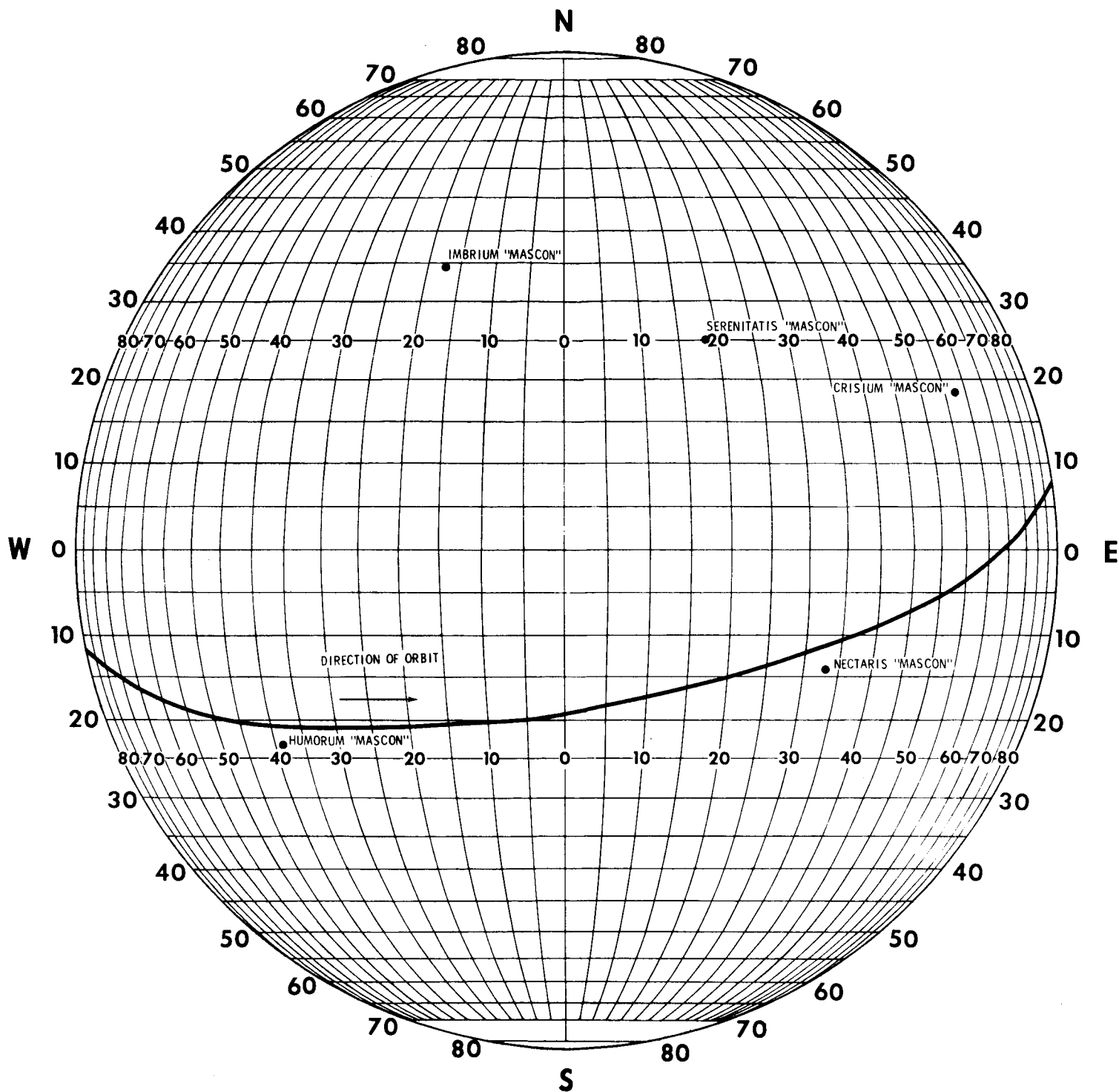


FIGURE 4 - GROUND TRACK FOR TRAJECTORY USED IN FIVE 'MASCON' STUDY

FIGURE 4A - EFFECT OF SINGLE "MASCON" ON DOPPLER OBSERVABLE -
TRAJECTORY 1 ($\lambda = 10^0$)

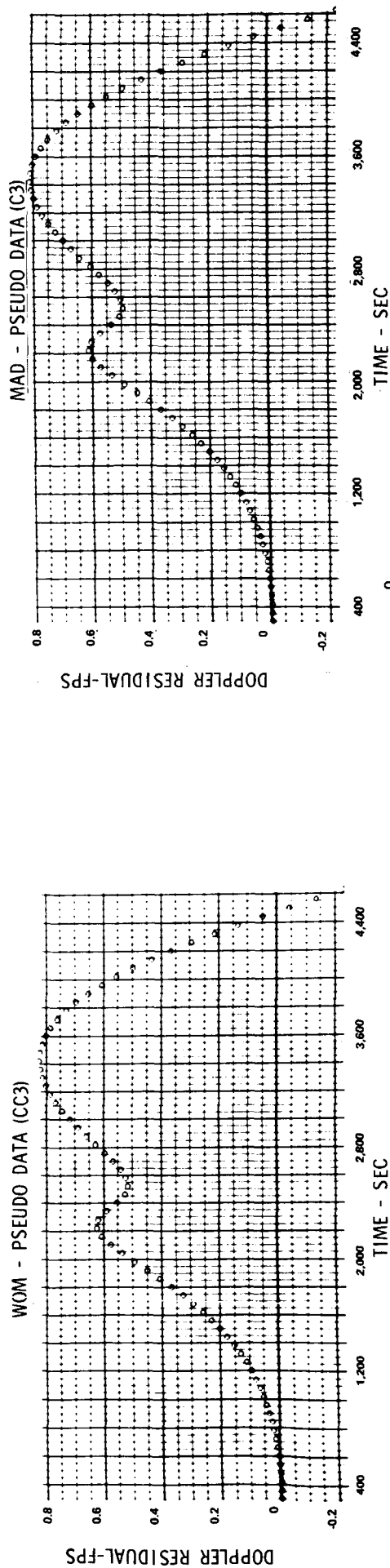


FIGURE 4B - FIT RESIDUALS - TRAJECTORY 1 ($\lambda = 10^0$)

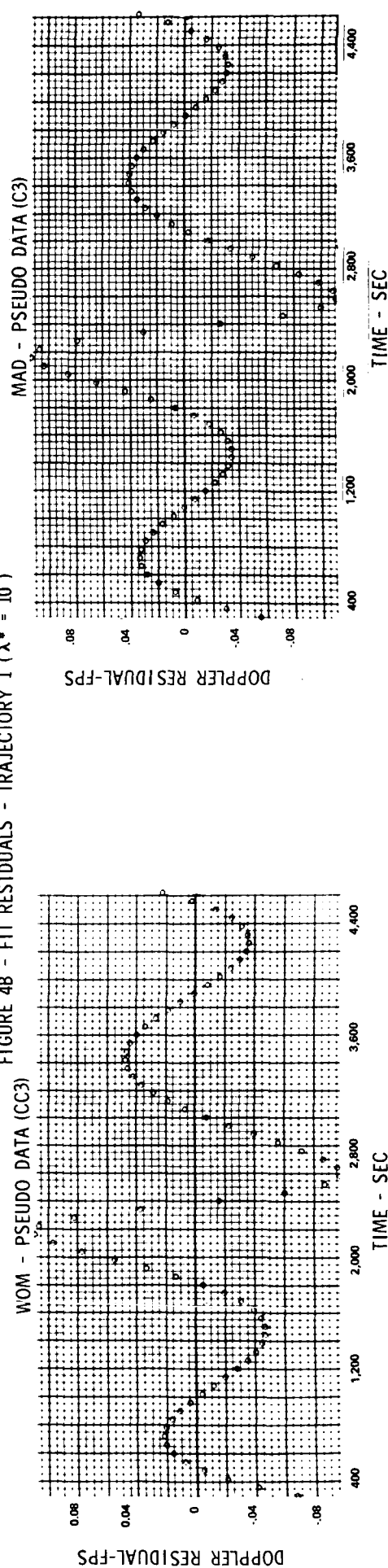


FIGURE 5A - EFFECT OF SINGLE "MASCON" ON DOPPLER OBSERVABLE -
TRAJECTORY 2 ($\lambda^* = 50^\circ$)

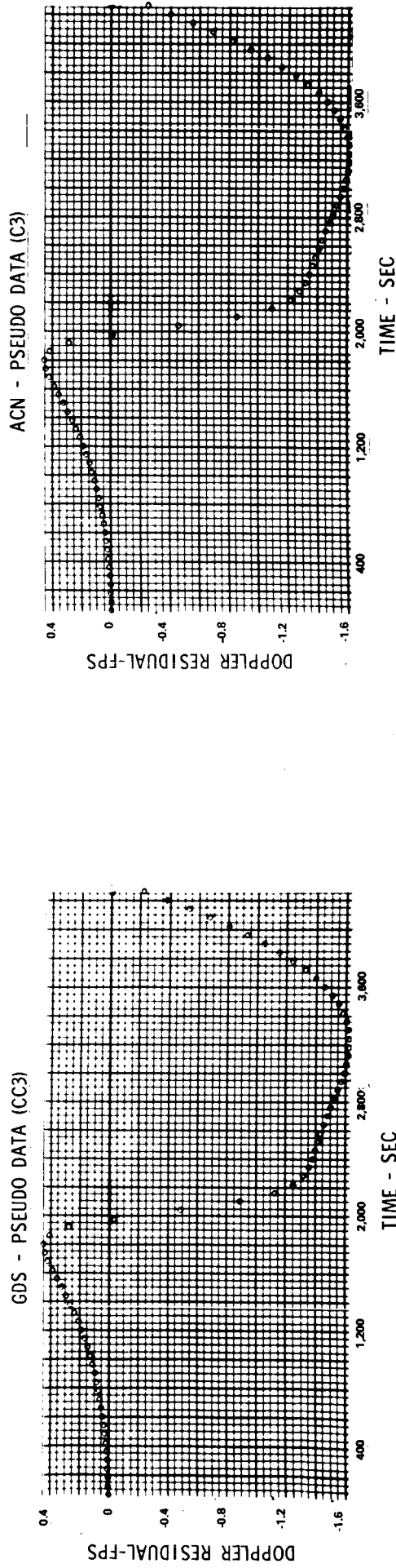


FIGURE 5B - FIT RESIDUALS - TRAJECTORY 2 ($\lambda^* = 50^\circ$)

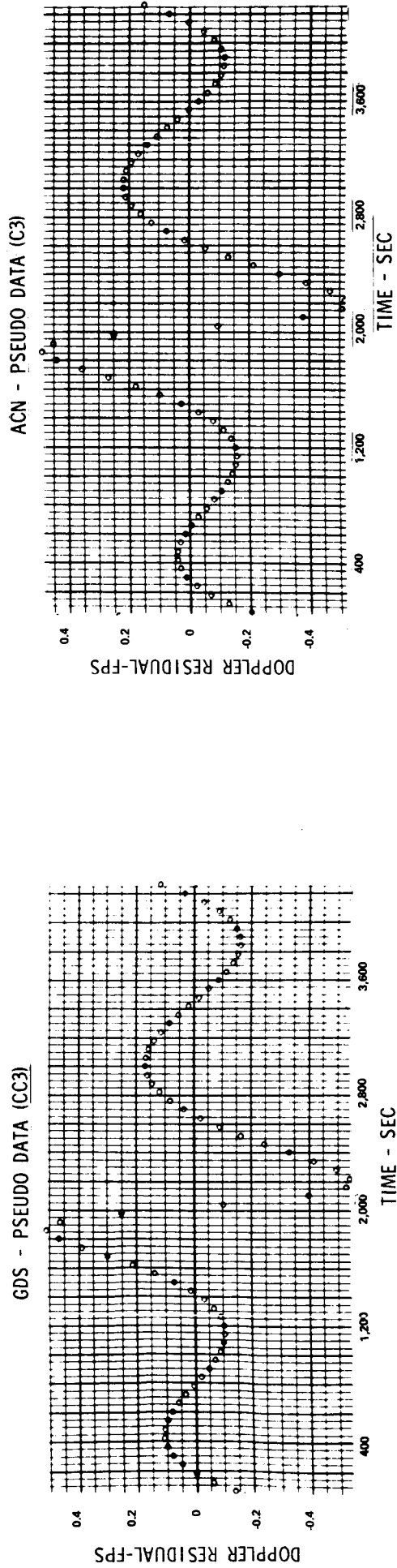


FIGURE 6A - EFFECT OF SINGLE "MASCON" ON DOPPLER OBSERVABLE -
TRAJECTORY 3 ($\lambda^* = 0^0$)

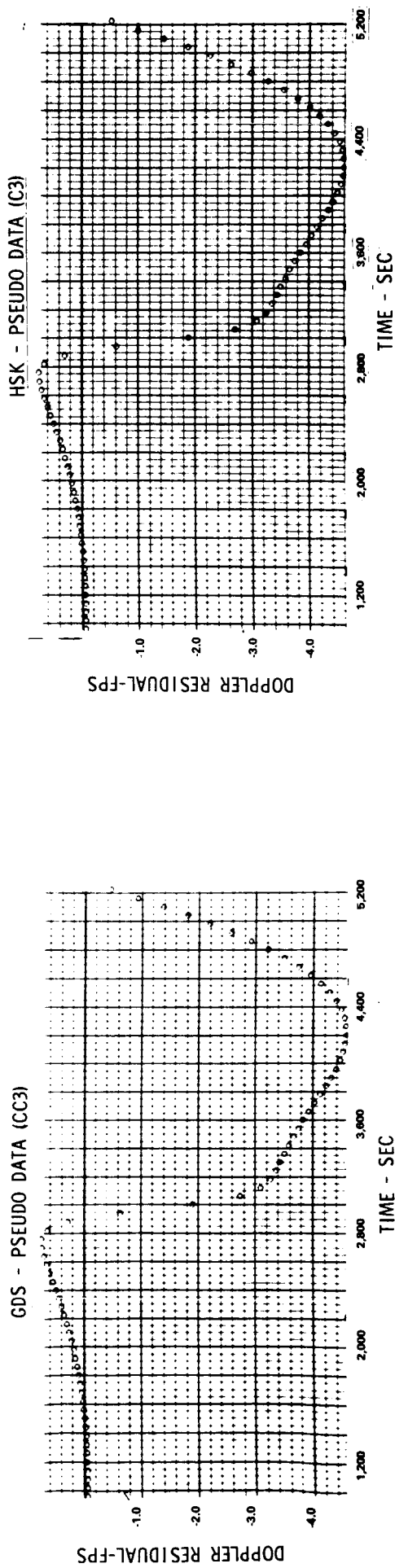


FIGURE 6B - FIT RESIDUALS - TRAJECTORY 3 ($\lambda^* = 0^0$)

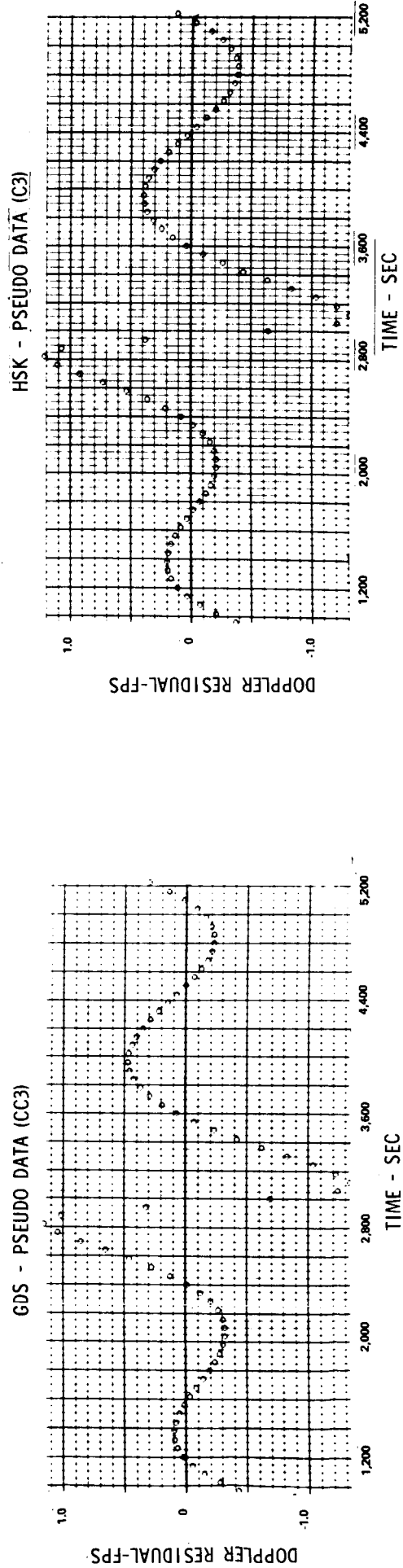
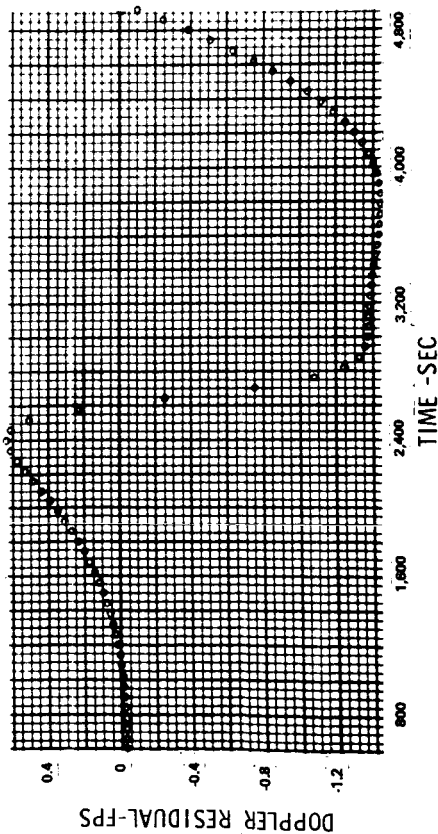


FIGURE 7A - EFFECT OF SINGLE "MASCON" ON DOPPLER OBSERVABLE -
TRAJECTORY 4 ($\lambda^* = -5^0$)

MAD - PSEUDO DATA (CC3)



CRO - PSEUDO DATA (C3)

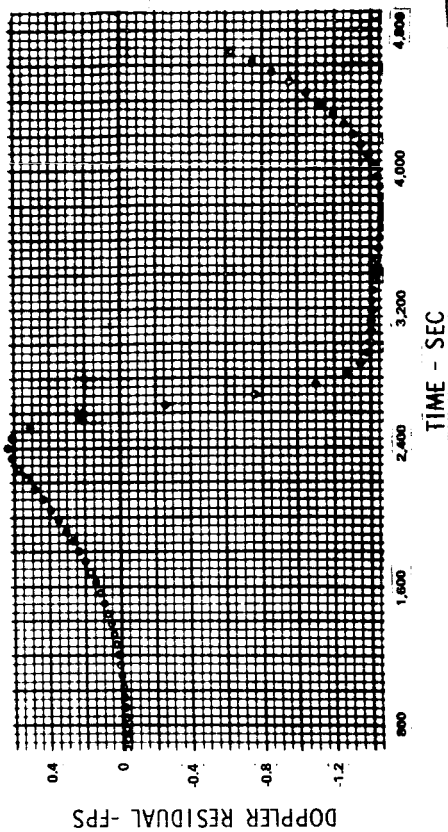
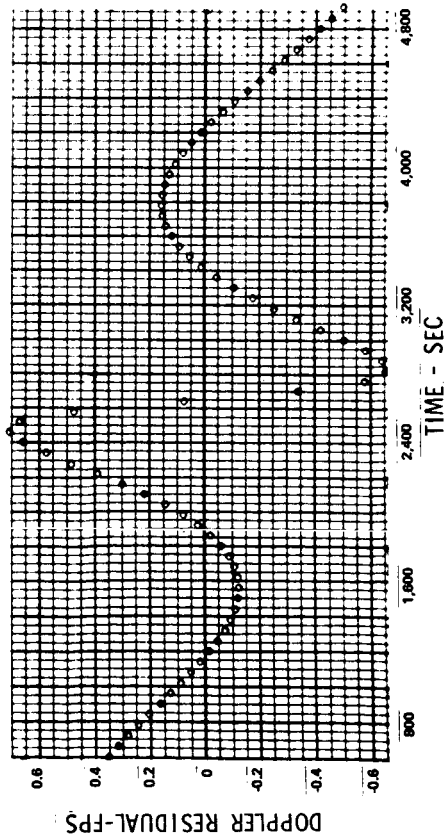


FIGURE 7B - FIT RESIDUALS - TRAJECTORY 4 ($\lambda^* = -5^0$)

MAD - PSEUDO DATA (CC3)



CRO - PSEUDO DATA (C3)

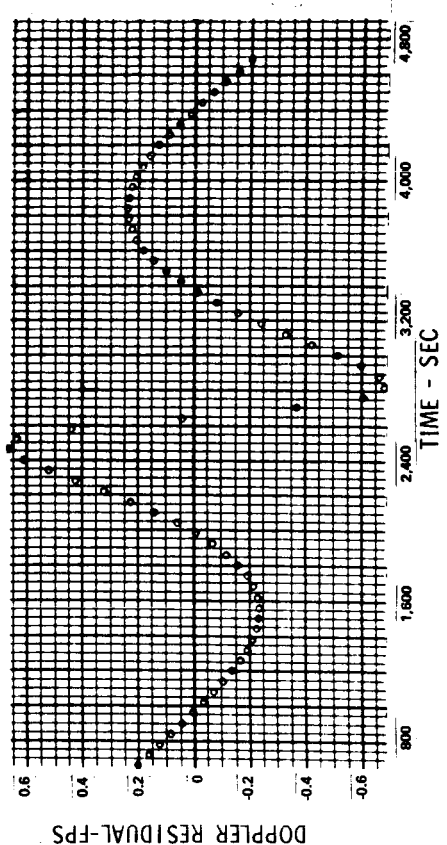


FIGURE 8A - EFFECT OF SINGLE "MASCON" ON DOPPLER OBSERVABLE -
TRAJECTORY 5 ($\lambda = -10^0$)

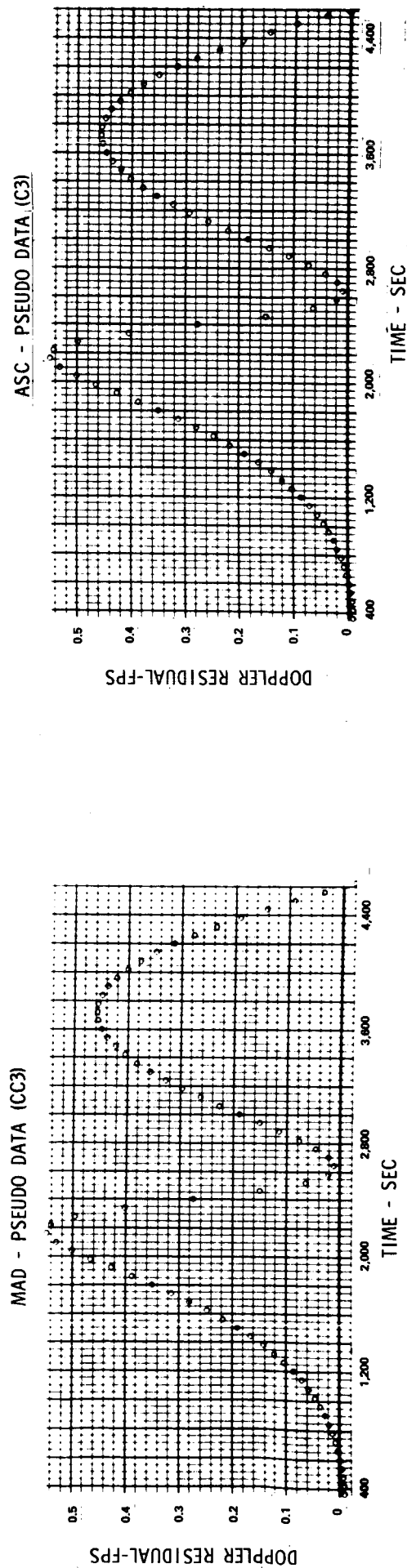


FIGURE 8B - FIT RESIDUALS - TRAJECTORY 5 ($\lambda = -10^0$)

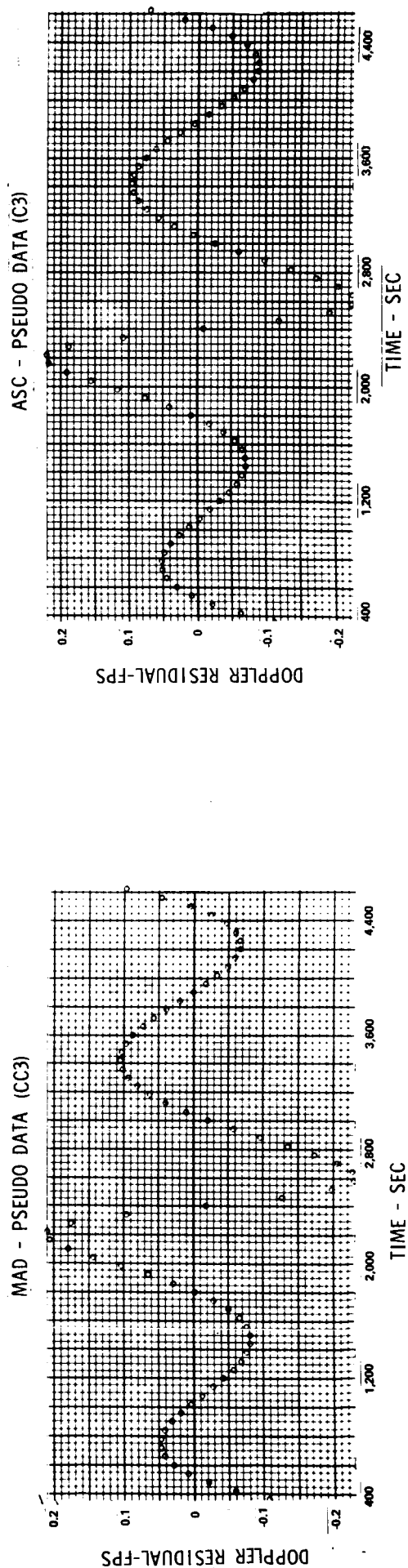


FIGURE 9A - EFFECT OF SINGLE "MASCON" ON DOPPLER OBSERVABLE -
TRAJECTORY 5A ($\lambda^* = -10^0$)

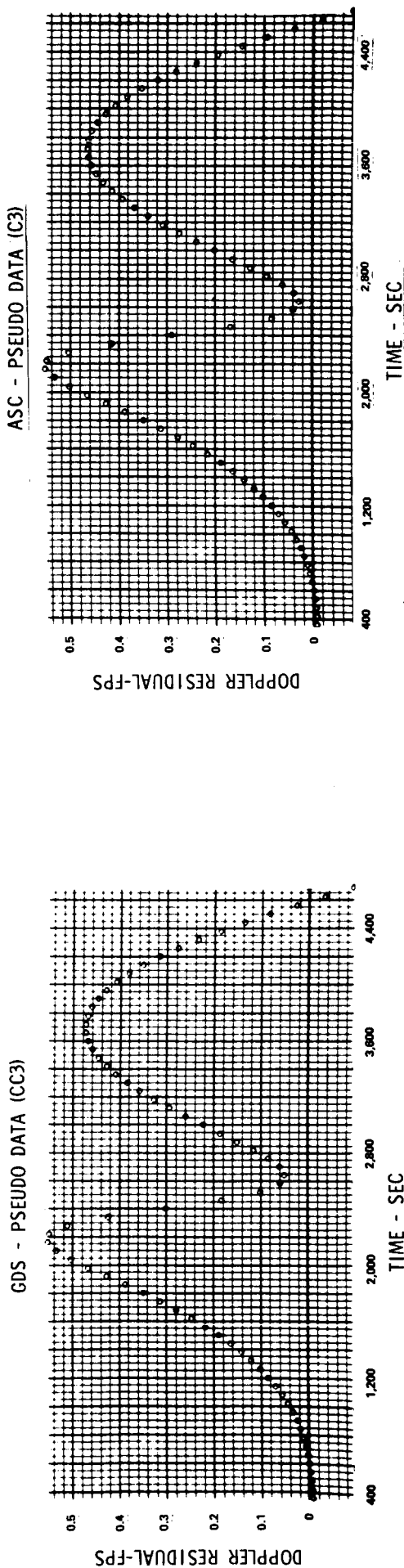
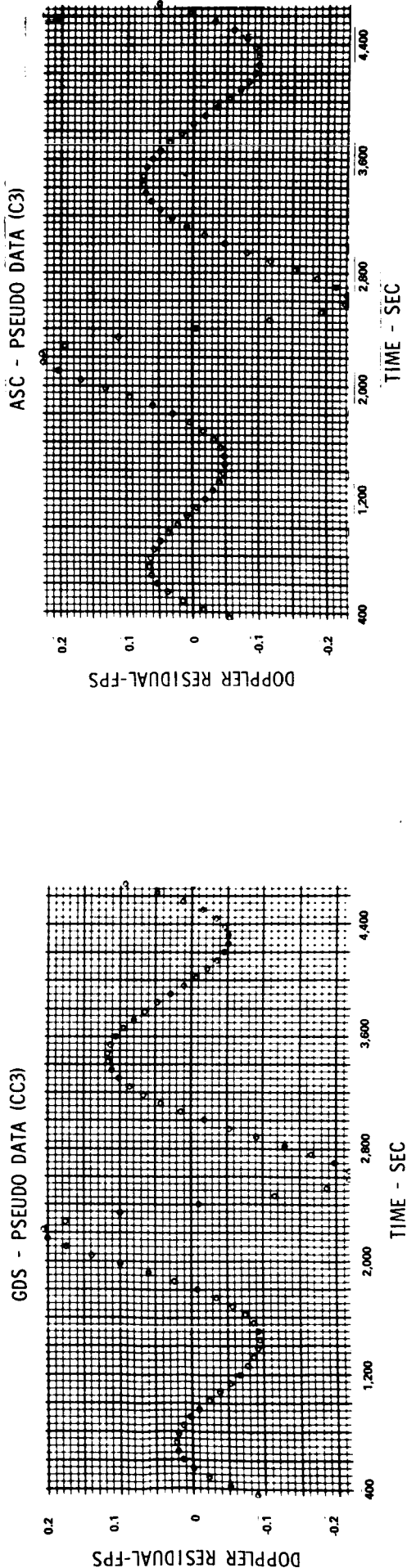


FIGURE 9B - FIT RESIDUALS - TRAJECTORY 5A ($\lambda^* = -10^0$)



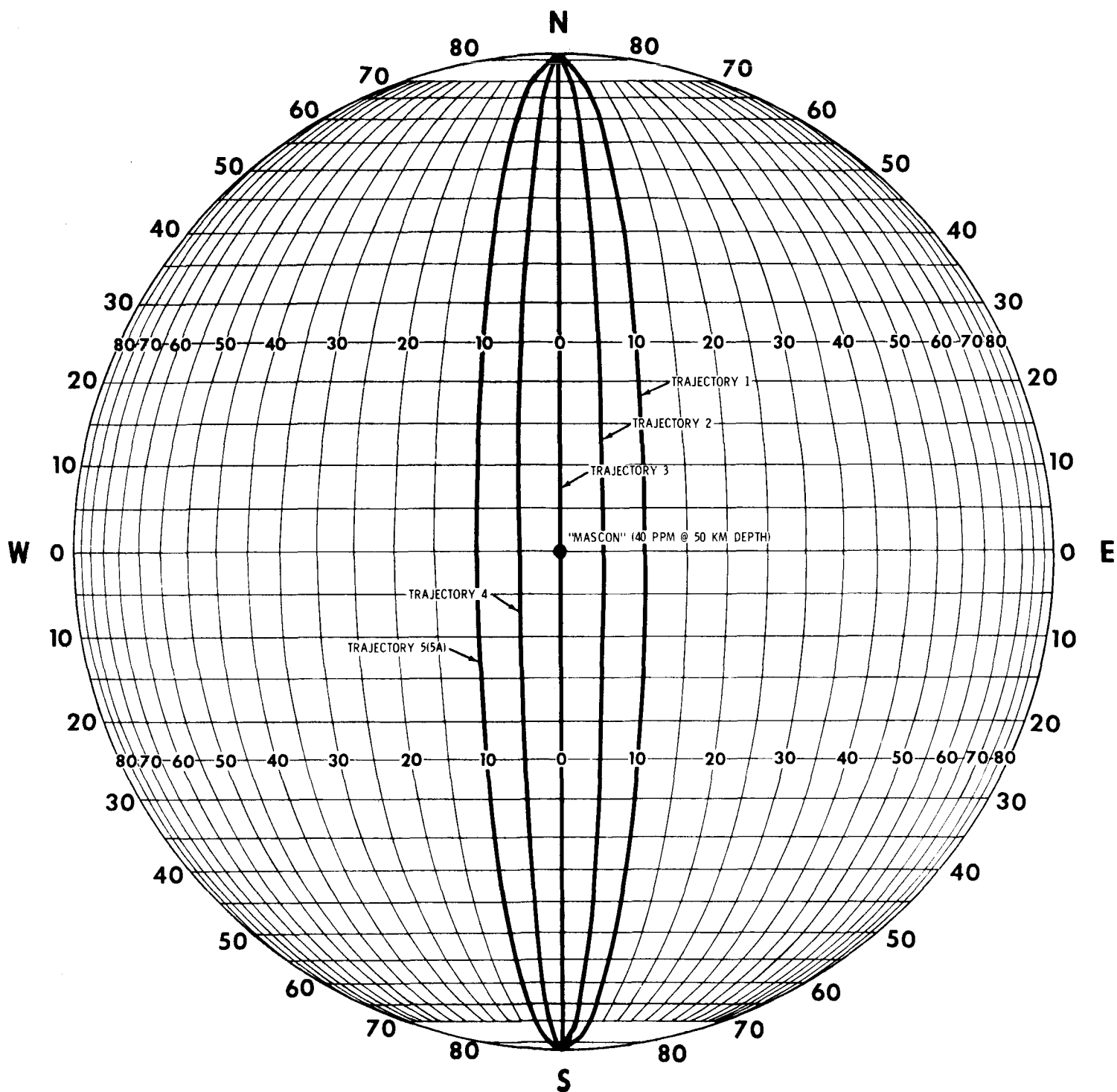


FIGURE 10 - GROUND TRACKS FOR TRAJECTORIES USED IN SINGLE "MASCON" STUDY

BELLCOMM, INC.

Subject: Addition of "Mascons" in BCMTAP and
a Preliminary Analysis of their
Effects on Orbit Determination
Case 310

From: J. T. Findlay

DISTRIBUTION LIST

Complete Memorandum to

NASA Headquarters

G. H. Hage/MA
T. A. Keegan/MA-2
S. C. Phillips/MA

GSFC

J. Barsky/554

LaRC

W. H. Michael, Jr./152A
R. H. Tolson/152A

MSC

J. P. Mayer/FM
J. C. McPherson/FM4
E. Schiesser/FM4
W. Wollenhaupt/FM4

BTL

W. M. Boyce/MH

JPL

P. Gottlieb/233-307
J. Lorell/156-217
P. Mueller/198-112A
W. L. Sjogren/180-304

Computer Usage Company

W. Ferguson
E. Fritz (5)
H. Lechner
J. Morris

Complete Memorandum to

Bellcomm, Inc.

D. R. Anselmo
A. P. Boysen, Jr.
J. O. Cappellari, Jr.
D. A. Corey
J. P. Downs
W. W. Ennis
C. L. Greer
D. R. Hagner
W. G. Heffron
T. B. Hoekstra
B. T. Howard
D. B. James
S. L. Levie, Jr.
M. Liwshitz
D. D. Lloyd
W. I. McLaughlin
J. Z. Menard
V. S. Mummert
B. G. Niedfeldt
D. H. Novak
F. N. Schmidt
R. V. Sperry
C. C. Tang
W. B. Thompson
J. W. Timko
J. E. Volonte
R. L. Wagner
All Members Department 2014
Department 1024 Files
Center 10 Files
Central Files
Library

← COPY TO

Abstract Only to

Bellcomm, Inc.

I. M. Ross